

Interaction of α - and β -Oligoarginine-Acids and Amides with Anionic Lipid Vesicles: A Mechanistic and Thermodynamic Study[†]

Thomas Hitz,^{‡,||} Rico Iten,[‡] James Gardiner,[§] Kenji Namoto,^{§,⊥} Peter Walde,^{*,‡} and Dieter Seebach[§]

Department of Materials, Institute of Polymers, and Department of Chemistry and Applied Biosciences, Laboratory of Organic Chemistry, ETH-Zürich, Wolfgang-Pauli-Strasse 10, CH-8093 Zürich, Switzerland

Received February 10, 2006; Revised Manuscript Received March 20, 2006

ABSTRACT: The interaction of α - and β -oligoarginine amides and acids and of α -polyarginine with anionic lipid vesicles was studied. The β -oligoarginines used were β^3 -homologues of the α -oligoarginines. Lipid bilayers were composed of POPC (1-palmitoyl-2-oleoyl-*sn*-glycero-3-phosphocholine) and POPG (1-palmitoyl-2-oleoyl-*sn*-glycero-3-[phospho-*rac*-(1-glycerol)]) containing 5 mol % pyrene-PG (1-hexadecanoyl-2-(1-pyrenedecanoyl)-*sn*-glycero-3-[phospho-*rac*-1-glycerol]). Kinetic analysis of the binding process onto large unilamellar POPC/POPG (3:7, molar ratio) vesicles (100 nm diameter) shows biphasic time courses for all tested peptides. The first binding step is fast and takes place within ~ 10 s with no disruption of the membrane as indicated by corresponding calcein release measurements. The second binding phase is slow and occurs within the next 30–300 s with substantial membrane disruption. In this context, β -hexa- and octaarginine amides possess higher second half-times than the β -hexa- and octaarginine acids of the same chain length. Furthermore β -octaarginine amide induces a calcein release approximately twice as large as that of the β -octaarginine acid. Thermodynamic analysis of the binding process, using the complex formation model that assumes that each peptide binds independently to n POPG lipids, reveals apparent binding constants (K_{app1}) of $\sim 5 \times 10^6 - 10^8 \text{ M}^{-1}$ and n -values from 3.7 for β -hexaarginine acid up to 24.8 for α -polyarginine. Although the K_{app1} -values are similar, the number of binding sites clearly depends on the chemical nature of the oligoarginine: β -oligoarginine amides and α -oligoarginine acids interact with more lipids than β -oligoarginine acids of the same length. Calculation of the electrostatic contribution to the total free energy of binding reveals that for all oligoarginines only 25–30% has electrostatic origin. The remaining ~ 70 –75% is nonelectrostatic, corresponding to hydrogen bonding and/or hydrophobic interactions. From the obtained data, a mechanism is suggested by which oligoarginines interact with anionic vesicles: (1) initial electrostatic interaction that is fast, nonspecific, and relatively weak; (2) nonelectrostatic interaction that is rate-limiting, stronger, and induces bilayer rigidification as well as release of aqueous contents from the vesicles.

Developing technologies that allow the enhanced transport of hydrophilic and charged molecules across the hydrophobic plasma membrane into living cells are of substantial interest for biomedical applications such as the delivery of genes or proteins (1, 2). Cell-penetrating peptides (CPPs¹, for a recent review see ref 3) belong to a class of oligopeptides that efficiently mediate the transport of extracellular cargo into cells. Such transport properties were demonstrated during the past decade for a number of hydrophilic molecules such as oligonucleotides, RNA, short interfering RNA, peptides, proteins, and even vesicles (4–7).

Two of the best-characterized CPPs are the Tat₄₈₋₆₀-transduction domain derived from the transcriptional activator of the HIV-1 virus and the *Drosophila* Antennapedia homeodomain peptide, penetratin (8, 9). Both peptides have a high proportion of arginine residues in their sequence. Recent reports show that the guanidine-moiety of the arginine-residue is critical to observe substantial peptide internalization: (i) replacing all nonarginine residues in Tat with arginine resulted in superior cellular uptake (factor of 20–100) (10); (ii) oligoarginines enter cells more efficiently than cationic homopolymers of lysine, ornithine, and histidine of the same length (11); (iii) inverting the absolute configuration of the arginine residues in the peptide chain does not affect cellular uptake (12); (iv) arginine-rich β -peptides and β -oligoarginines efficiently permeate into mammalian and bacterial cells (13–16); and (v) even highly branched guanidinoglycosides and guanidinium-rich dendrimers are transported across the plasma membrane (17–18). It has also been shown that branched octaarginine is internalized to the same extent as linear octaarginine (19). In the case of fluorescein-labeled amide derivatives of β -oligoarginines, it has been shown that a chain length of ≥ 7 leads to efficient

[†] J.G. acknowledges financial support from a New Zealand Foundation for Research Science and Technology postdoctoral fellowship (No. SWISS0401). K.N. acknowledges partial financial support from the Swiss National Science Foundation (SNF Project 20020-100 182).

* To whom correspondence should be addressed: Telephone: +41-6320473. Fax: +41-6321265. E-mail: peter.walde@mat.ethz.ch.

[‡] Department of Materials, Institute of Polymers, ETH-Zürich.

[§] Department of Chemistry and Applied Biosciences, Laboratory of Organic Chemistry, ETH-Zürich.

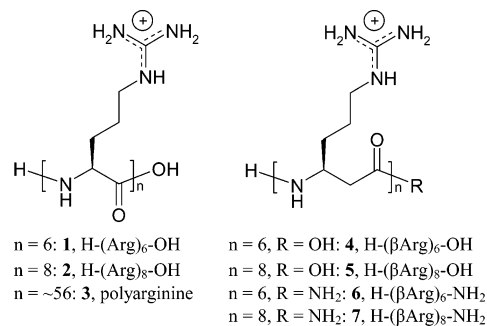
^{||} Present address: Mettler-Toledo GmbH, 8603 Schwerzenbach, Switzerland.

[⊥] Present address: Novartis Pharma AG, NIBR, 4002 Basel, Switzerland.

cell uptake (14). Corresponding cell uptake data for free acids are not available.

Despite the importance of CPPs as efficient delivery vectors and the important role of the guanidinium-moiety for peptide transduction, the mechanisms of cellular uptake remain elusive. It has become increasingly clear that more than one mechanism is responsible for peptide internalization depending on the chemical nature of the peptides and cell lines. In general, two different pathways are observed, endocytotic and/or nonendocytotic uptake. Internalization studies with live cells and bacterial cells lacking the possibility of endocytosis suggest that α - and β - oligoarginines use alternative mechanisms to the endocytotic uptake (15, 20, 21). Wender and co-workers (22) proposed a possible nonendocytotic pathway that could explain such observations. It is argued that first the oligoarginines form bidentate hydrogen bonds with H-bond acceptors on the cell surface. These complexes are assumed to partition into, and migrate across, the membrane bilayer proportional to the membrane potential. This conclusion is compatible with the observed increased uptake of H-(D-Arg)₈-OH with increased membrane potential. Recent studies indicate that complex formation between oligoarginines and cell surface proteoglycans (i.e., heparan sulfate) is favored over a peptide binding onto anionic lipids (23, 24). However, in an endocytotic pathway where heparan sulfate is degraded by heparanases, hydrogen bonding with anionic lipids on the inner leaflet of the endocytotic vesicle may become more important in allowing the peptide and its cargo to escape. For example, it has been shown that anionic lipids such as phosphatidylserine mediate the release of DNA from cationic liposome/DNA complexes in the endosomal compartment (25). Interactions with anionic phospholipids may also play an important role in the observed uptake of oligoarginines into Gram-negative bacterial cells, since the inner membrane contains POPE (1-

Scheme 1: Chemical Structures of the α - and β^3 -oligoarginine Amides and Acids Used in This Study



palmitoyl-2-oleoyl-*sn*-glycero-3-phosphoethanolamine) and negatively charged POPG (1-palmitoyl-2-oleoyl-*sn*-glycero-3-[phospho-*rac*-(1-glycerol)]) but lacks proteoglycans (15, 26).

In the present study, we investigate the interaction of α - and β -oligoarginine amides and of the corresponding acids (Scheme 1, 1–7), with anionic lipid vesicles composed of POPC (1-palmitoyl-2-oleoyl-*sn*-glycero-3-phosphocholine) and POPG. By using pyrene-labeled PG-lipids (pyrene-PG, 1-hexadecanoyl-2-(1-pyrenedecanoyl)-*sn*-glycero-3-[phospho-*rac*-1-glycerol]) and encapsulated calcein, we compared the interaction of oligoarginines 1–7 on a thermodynamic and mechanistic level, as studied by fluorescence spectroscopy. Pyrene-labeled phospholipids have previously been used to monitor the interaction of several proteins and peptides with anionic vesicles (27–30). These probes respond in a characteristic manner to phase separation and changes in the lateral mobility of phospholipids caused by peptide association (31). Circular dichroism (CD) spectroscopy was applied to monitor possible structural changes of the vesicles-bound peptides.

MATERIALS AND METHODS

Lipids, Peptides, and General Chemicals. POPC and POPG were purchased from Avanti Polar Lipids (Alabaster, AL); pyrene-PG was from Molecular Probes (Eugene, OR). Calcein (for fluorescence), 4-(2-hydroxyethyl)piperazine-1-ethanesulfonic acid sodium salt (HEPES-Na), sodium chloride (NaCl), ethylenediaminetetraacetic acid disodium salt dihydrate (EDTA disodium salt), and Triton X-100 were purchased from Sigma Aldrich (Buchs, Switzerland). Peptide 1 (> 88%, supplied as trifluoroacetate salt) was from Bachem (Bubendorf, Switzerland). Peptides 2 and 4–7 were prepared using Fmoc solid-phase peptide synthesis (> 98%, trifluoroacetate salts) (14, 32, 33; see below and Supporting Information). Peptide 3 (polyarginine, poly-L-arginine hydrochloride, P-4663, Lot 122K5116; degree of polymerization and relative molar mass as determined by multi angle laser light scattering measurements, 39 and 7540, respectively; degree of polymerization and relative molar mass as determined by viscosity measurements, 72 and 14 000) was from Sigma Aldrich (Buchs, Switzerland). For peptide 3, an average degree of polymerization of 56, corresponding to a relative molar mass of 10 770 was used for concentration calculations.

Synthesis of Peptides 2 and 4–7. For a general article on β -peptides and their nomenclature, see ref 33. In the text of this paper, the short form descriptions for the peptides are

¹ Abbreviations: CPP, cell penetrating peptide; POPC, 1-palmitoyl-2-oleoyl-*sn*-glycero-3-phosphocholine; POPG, 1-palmitoyl-2-oleoyl-*sn*-glycero-3-[phospho-*rac*-(1-glycerol)]; pyrene-PG, 1-hexadecanoyl-2-(1-pyrenedecanoyl)-*sn*-glycero-3-[phospho-*rac*-1-glycerol]; HEPES, 4-(2-hydroxyethyl)piperazine-1-ethanesulfonic acid; EDTA, ethylenediaminetetraacetic acid; LUV, large unilamellar vesicle; CD, circular dichroism; DLS, dynamic light scattering; Cryo-TEM, cryo transmission electron microscopy; RFI_M, fluorescence intensity of the pyrene-PG monomer in the presence of peptides relative to the fluorescence intensity of the pyrene-PG monomer in the absence of peptides; RFI_E, fluorescence intensity of the pyrene-PG excimer in the presence of peptides relative to the fluorescence intensity of the pyrene-PG excimer in the absence of peptides; I_M, fluorescence intensity of pyrene-PG monomer; I_E, fluorescence intensity of pyrene-PG excimer; ΔI_F , observed increase in fluorescence intensity; ΔI_{Fmax} , observed maximal increase in fluorescence intensity; P, peptide; [P]_{tot}, total peptide concentration; [P], concentration of peptide in the bulk solution; L, accessible negatively charged phospholipid (POPG); [L]_{tot}, total concentration of accessible, negatively charged phospholipids (POPG molecules present in the outer leaflet of the bilayer); n, number of negatively charged phospholipids bound to one peptide; [L_n], concentration of accessible peptide binding sites, composed of n negatively charged phospholipids; [L_n]_{tot}, total concentration of accessible binding sites for the peptide; [P × L_n], concentration of bound peptide, equal to the concentration of occupied peptide binding sites; [M]_{tot}, total concentration of accessible membrane lipids (POPC + POPG present in the outer layer of the vesicles); K_{app1}, apparent binding constant for peptide binding to peptide-free (charged) vesicles; K_{app2}, apparent binding constant for peptide binding to vesicles that are just saturated with peptides (no surface charge); SD, standard deviation; peptide 1, H-(Arg)₆-OH; peptide 2, H-(Arg)₈-OH; peptide 3, polyarginine; peptide 4, H-(β Arg)₆-OH; peptide 5, H-(β Arg)₈-OH; peptide 6, H-(β Arg)₆-NH₂; peptide 7, H-(β Arg)₈-NH₂.

used, for example, H-(β Arg)₆-OH (**4**) which is H-(β^3 hArg)₆-OH (**4**) (see below).

1. Abbreviations Used for This Section. F, flow rate; HPLC, high-performance liquid chromatography; MALDI, matrix-assisted laser desorption ionization; TFA, trifluoroacetic acid. Anal. reversed-phase (RP) HPLC: Merck/Hitachi HPLC system (LaChrom, L-7150 pump, UV detector L-7400, Interface D-7000). Column: Nucleosil 100-5 C18 (250 \times 4 mm, Macherey-Nagel). HPLC analysis: with a linear gradient of A (0.1% TFA in H₂O) and B (acetonitrile) at a flow rate of 1 mL \cdot min⁻¹ with UV detection at 220 nm. Retention time (t_R) in minutes. Prep. reversed-phase (RP) HPLC: Merck/Hitachi HPLC system (LaChrom, L-7150 pump, UV detector L-7400, Interface D-7000). Column: Nucleosil 100-7 C18 (250 \times 21 mm, Macherey-Nagel). Crude products were purified with a gradient of A (0.1% TFA in H₂O) and B (acetonitrile) at a flow rate of 17 mL \cdot min⁻¹, with UV detection at 220 nm, and subsequently lyophilized (Hetosicc cooling condenser with a hi-vacuum pump). UV-grade TFA (>99% GC) was used for RP-HPLC.

2. Peptides 2, 4, and 5. H-(Arg)₈-OH (**2**), H-(β^3 hArg)₆-OH (**4**), and H-(β^3 hArg)₈-OH (**5**) were prepared by solid-phase peptide synthesis (SPPS) using Wang resin and Fmoc-protecting group strategy in a manner similar to that previously described for the corresponding amide derivatives (**14**); see Supporting Information for details.

2.1 H-(Arg)₈-OH (2). A total of 66 mg of the crude peptide TFA salt of **2** was purified by RP-HPLC (5% B for 5 min, 5–15% B in 30 min, $F = 17$ mL \cdot min⁻¹) to give 8.1 mg of pure H-(Arg)₈-OH (**2**) as a TFA salt, white solid. RP-HPLC (5% B for 5 min, 5–15% B in 30 min): $t_R = 18.7$, purity > 98%. ESI-MS 1266.01 (M – H), MALDI-MS 1291.8 (12), 1290.8 (18), 1289.8 (36, [M + Na]⁺), 1269.8 (19), 1268.8 (68), 1267.8 (100, [M + H]⁺). HR-MS: 1267.8290 ([C₄₈H₉₈N₃₂O₉]⁺; calcd 1267.8273).

2.2 H-(β^3 hArg)₆-OH (4). A total of 55 mg of the crude peptide TFA salt of **4** was purified by RP-HPLC (5% B for 5 min, 5–15% B in 30 min, $F = 17$ mL \cdot min⁻¹) to give 14 mg of pure H-(β^3 hArg)₆-OH (**4**) as a TFA salt, white solid. RP-HPLC (5% B for 5 min, 5–15% B in 30 min): t_R 16.5, purity > 98%. MALDI-MS 1178.1 (10, [M + K]⁺), 1062.7 (11, [M + Na]⁺), 1061.7 (23), 1041.7 (17), 1040.7 (51), 1039.7 (100, [M + H]⁺), 1022.7 (22), 980.7 (10), 844 (6), 764 (7), 661.0 (10), 520.9 (11), 520.4 (17), 506.0 (16), 456.0 (20), 413.3 (14), 317.0 (17). HR-MS: 1039.7184 ([C₄₂H₈₇N₂₄O₇]⁺; calcd 1039.7189).

2.3 H-(β^3 hArg)₈-OH (5). A total of 130 mg of the crude peptide TFA salt of **5** was purified by RP-HPLC (5% B for 5 min, 5–15% B in 30 min, $F = 17$ mL \cdot min⁻¹) to give 32 mg of pure H-(β^3 hArg)₈-OH (**5**) as a TFA salt, white solid. RP-HPLC (5% B for 5 min, 5–15% B in 30 min): t_R 27.3, purity > 98%. MALDI-MS 1403.9 (3.5), 1402.9 (8), 1401.9 (10, [M + Na]⁺), 1382.0 (28), 1381.0 (72), 1380.0 (100, [M + H]⁺), 1363.9 (15), 1362.9 (21), 1321.9 (11), 1320.9 (15), 1279.9 (4), 1278.9 (6), 1262.8 (4), 1261.8 (6), 1245.8 (3), 1244.8 (4), 691.0 (2), 690.6 (2). HR-MS: 1379.9549 ([C₅₆H₁₁₅N₃₂O₉]⁺; calcd 1379.9525).

3. Peptides 6 and 7. Peptides H-(β^3 hArg)₆-NH₂ (**6**) and H-(β^3 hArg)₈-NH₂ (**7**) were prepared according to previously published procedures (**14**).

Preparation of Large 100 nm Unilamellar Vesicles (LUVs). Dried films of POPC and POPG (molar ratio = 3:7)

with 5 mol % pyrene-PG were hydrated with 5 mM HEPES, 0.1 mM EDTA, and 150 mM NaCl, pH 7.4, in a 25 mL round-bottom flask. A heterogeneous vesicle suspension was formed by vortexing. This suspension was frozen 10 times in liquid nitrogen (–195 °C) and thawed in a water bath at 40 °C. To decrease the vesicle size and lamellarity, the vesicle suspension was repeatedly passed through two Nucleopore polycarbonate membranes from Sterico AG (Dietikon, Switzerland) with mean pore diameters of 400 nm (10 times), 200 nm (10 times), and 100 nm (10 times) using The Extruder (from Lipex Biomembranes, Inc., Vancouver, Canada) (**34**). Homogeneous size distribution and unilamellarity of the obtained vesicles was confirmed by dynamic light scattering (DLS) and cryo transmission electron microscopy (cryo-TEM).

DLS and Cryo-TEM. DLS analysis was performed on a BI-200SM equipment from Brookhaven Instruments Limited, with an argon-ion laser (M95-2, Lexel) operating at a wavelength of 514.5 nm (green) or 488 nm (blue) and a goniometer in the angle range from 15 to 150°. Cryo-TEM analysis was carried out by Dr. Martin Müller at the Institute of Applied Physics, Department of Physics, ETH Zürich, as previously described (**35**). The analyzed vesicles had a diameter between 90 and 120 nm, and their size was stable for at least 2 month in buffer (5mM HEPES, 0.1 mM EDTA, and 150 mM NaCl, pH 7.4).

Fluorescence Measurements. Fluorescence measurements were performed on a Spex Fluorolog 2 instrument from Jobin Yvon (U.K.) using 1 cm quartz cells equipped with a magnetic stirrer bar and thermostated at 25 °C. In general, prior to the peptide addition, the cells were filled with the appropriate vesicle suspensions and incubated under stirring in the dark at 25 °C for at least 10 min.

Kinetic Analysis of Peptide Binding. A volume of 5 μ L of concentrated peptide solutions (0–2.4 mM) was added under constant stirring to 3 mL of POPC/POPG vesicle suspensions (molar ratio = 3:7, 10 μ M with 5 mol % pyrene-PG), and the measurement was immediately started. All experiments were performed in 5 mM HEPES, 0.1 mM EDTA, and 150 mM NaCl, pH 7.4. The excitation wavelength (λ_{ex}) was 344 nm and the emission wavelength (λ_{em}) 376 nm (signal of the pyrene-PG monomer). The fluorescence intensity reported in the figures is relative to the fluorescence intensity in the absence of peptides: RFI_M.

The observed biphasic fluorescence increase with time was fit with the following equation that contains two exponential terms for two consecutive first-order processes (see Supporting Information):

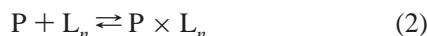
$$F(t) = A_1[1 - \exp(-k_1t)] + A_2[1 - \exp(-k_2t)] + F_0 \quad (1)$$

where $F(t)$ is the measured fluorescence as a function of time and F_0 the measured fluorescence at time = 0 s; k_1 and k_2 are the rate constants for the fast and the slow phases. The corresponding half-times $t_{1/2-i}$ are given by $\ln 2/k_i$, with $i = 1, 2$. A_1 and A_2 represent the amplitudes of the fast and slow phases. Curve fitting was performed using nonlinear least-squares regression and the Software Origin from OriginLab Corp. (Northampton, MA).

Calculation of the Excimer to Monomer Ratio of Pyrene Fluorescence. Directly after the kinetic measurements, emission-spectra of peptide-containing vesicle suspensions were

recorded ($\lambda_{\text{ex}} = 344$ nm, $\lambda_{\text{em}} = 360\text{--}520$ nm). The fluorescence-intensity ratio $I_{482\text{nm}}/I_{376\text{nm}}$ was utilized to monitor the excimer-to-monomer ratio of pyrene in pyrene-PG as a function of the peptide concentration. Presented excimer-to-monomer ratios are expressed relative to the signal in absence of peptide: $\text{RFI}_E/\text{RFI}_M$.

Thermodynamic Analysis with the Complex Formation Model. The maximum of the fluorescence increase observed in the kinetic measurements (ΔI_{Fmax}) was averaged over 20 s for each peptide concentration. These ΔI_{Fmax} -values were utilized to monitor the binding onto the anionic POPC/POPG vesicles at equilibrium. We assume that oligoarginines attach only to negatively charged POPG and only the outer leaflet of the bilayer is available for binding ($\cong 54\%$ of the total POPG present in 100 nm-vesicles). The apparent constant of binding (K_{app1}) was calculated for the following complex formation model (31, 36):



where P stands for peptide, L for the negatively charged phospholipid POPG, and n for the number of POPG-lipids bound to one peptide. Therefore, the binding site to which one peptide binds consists of n POPG-lipids. $\text{P} \times \text{L}_n$ is the complex formed between one peptide and n POPG molecules. The equilibrium constant K_{app1} (M^{-1}) is given by the following equation:²

$$K_{\text{app1}} = \frac{[\text{P} \times \text{L}_n]}{[\text{P}] \times [\text{L}_n]} \quad (3)$$

It is assumed that the observed increase in pyrene fluorescence (ΔI_{F}) divided by the maximally observed fluorescence change (ΔI_{Fmax}) is directly proportional to the concentration of the binding sites occupied divided by the concentration of all available binding sites. This leads to the following relationship (31):

$$\frac{\Delta I_{\text{F}}}{\Delta I_{\text{Fmax}}} = \frac{[\text{P} \times \text{L}_n]}{[\text{L}_n]_{\text{tot}}} \quad (4)$$

$[\text{P} \times \text{L}_n]$ corresponds to the concentration of bound peptide, which is equal to the concentration of occupied binding sites. $[\text{L}_n]_{\text{tot}}$ corresponds to the concentration of all accessible binding sites and is equal to $[\text{L}]_{\text{tot}}/n$. In this study, $[\text{L}]_{\text{tot}}$ is equal to the POPG concentration in the outer leaflet of the bilayer. The concentration of the unbound peptide [P] and the concentration of the available (un-occupied) binding sites $[\text{L}_n]$ during the binding process are given by the following mass balances:

$$[\text{P}] = [\text{P}]_{\text{tot}} - [\text{P} \times \text{L}_n] \quad (5)$$

$$[\text{L}_n] = [\text{L}_n]_{\text{tot}} - [\text{P} \times \text{L}_n] \quad (6)$$

When eqs 3–6 are combined, it is possible to evaluate (by fitting) K_{app1} and n by measuring ΔI_{F} and ΔI_{Fmax} and by

² Note that every thermodynamic equilibrium constant is defined by $\Delta G^\circ = -RT \ln K$, whereby the equilibrium constant K is without any units. However, for the sake of comparison with literature, all equilibrium constants defined in this work have units, e.g., for the peptide-vesicle binding equilibrium formulated with eq 2, the unit is M^{-1} .

knowing $[\text{L}]_{\text{tot}}$ and $[\text{P}]_{\text{tot}}$. $[\text{P}]_{\text{tot}}$ stands for the total peptide concentration. $[\text{P} \times \text{L}_n]$ can be calculated from K_{app1} and n for any given $[\text{P}]_{\text{tot}}$ and $[\text{L}]_{\text{tot}}$ (see Supporting Information). K_{app1} describes the binding of the peptides to peptide-free vesicles.

Thermodynamic Analysis with the Partitioning Model. For quantifying the interaction of the peptides with vesicles that already contain some bound peptides, the partitioning model was also considered (37). The peptide is assumed to partition between a bulk aqueous phase and a lipidic membrane phase (the outer layer of the vesicles). The degree of binding is defined as follows (38):

$$X_b = \frac{[\text{P} \times \text{L}_n]}{[\text{M}]_{\text{tot}}} \quad (7)$$

$[\text{M}]_{\text{tot}}$ is the total concentration of accessible membrane lipids (POPC + POPG present in the outer layer of the vesicles). X_b was plotted as a function of [P], the equilibrium concentration of the peptide in the bulk aqueous phase, and the apparent partition coefficient was calculated for conditions under which the vesicle surface was almost saturated with peptides, yielding the apparent partition coefficient

$$K_p = K_{\text{app2}} = \frac{X_b^{\text{sat}}}{[\text{P}]^{\text{sat}}} \quad (8)$$

For a direct comparison of K_{app2} with mole fraction partition coefficients, K_{app2} has to be multiplied by the factor 55.5 M (39).³

Calculation of the Effective Peptide Charge, z_p . The vesicle surface charge density (σ) of POPC/POPG membranes is given by (40)

$$\sigma = (e_0/A_L) \frac{-X_{\text{PG}}(1 - X_{\text{Na}^+}) + z_p \times X_b}{1 + (A_p/A_L) \times X_b} \quad (9)$$

Where e_0 is the elementary charge, A_L is the lateral cross sectional area per lipid molecule ($\sim 72 \text{ \AA}^2$ (41)), X_{PG} is the mole fraction of anionic POPG ($[\text{POPG}]/([\text{POPC}] + [\text{POPG}]) = 0.7$), X_{Na^+} is the mole fraction of Na^+ associated with POPG, z_p is the effective peptide charge, X_b is the degree of binding obtained from the complex formation model, and A_p is the effective area of the peptide at the membrane surface (assumed to be $\sim 100 \text{ \AA}^2$ (42)). X_{Na^+} is ≈ 0 , as calculated by assuming a Langmuir adsorption isotherm and an association constant of 0.6 M^{-1} for Na^+ to POPG (43); see Supporting Information.

Assuming that at the lowest total peptide concentration at which saturation is observed (no significant further change in fluorescence intensity observed after adding more peptide) the surface charge density (σ) is zero, z_p was calculated for the different peptides (see Supporting Information).

Calculation of the Nonelectrostatic Contribution to the Peptide Binding. For distinguishing electrostatic from

³ The mole fraction partition coefficient K_x is defined as X_b/X_w , where X_b and X_w are the mole fractions of the peptide in the membrane and in water, respectively. In the case of $K_{\text{app}} = X_b/[\text{P}]$, the equilibrium concentration of the peptide in water, [P], is given as a mole per liter solution containing 55.5 mol of water as the dominant species.

nonelectrostatic contributions to the binding, $\Delta G_{\text{nonelect}} = -RT \ln K_{\text{app}2}$ was calculated as well as $\Delta G_{\text{el}} = -RT \ln(K_{\text{app}1}/K_{\text{app}2})$ (38).

Vesicle Leakage. An 80 mM calcein solution in 5 mM HEPES, 0.1 mM EDTA, and 30 mM NaCl, pH 7.4, was added to a vacuum-dried lipid film composed of POPC and POPG (molar ratio = 3:7) and incubated for 5 min with shaking to entrap calcein in the formed vesicles. Vesicles homogeneous in size (100 nm in diameter on average) and unilamellar were prepared according to the method mentioned above. Vesicles with entrapped calcein were separated from nonentrapped calcein by size exclusion chromatography (Sephacrose 4B from Amersham Biosciences AB, Uppsala, Sweden) using 5 mM HEPES, 0.1 mM EDTA, and 150 mM NaCl, pH 7.4, as eluate buffer. The estimated entrapment yield was $\sim 1\%$ and the internal volume (V_{int}) $\sim 3.7 \text{ L mol}^{-1}$. Leakage experiments were performed by adding 5 μL of peptide solution to 3 mL 10 μM POPC/POPG vesicle suspension in 5 mM HEPES, 0.1 mM EDTA, and 150 mM NaCl, pH 7.4. Maximal leakage was determined by adding 5 μL of Triton X-100. Calcein release was determined by measuring the fluorescence intensity at 513 nm (excitation 496 nm), and %-leakage was calculated after 1200 s (arbitrarily chosen) according to

$$[(I_{1200} - I_0)/(I_{\text{Triton}} - I_0)] \times 100 \quad (10)$$

where I_{1200} denotes the fluorescence intensity determined after 1200 s, I_0 the intensity at $t = 0$ s, and I_{Triton} the intensity after adding Triton X-100.

CD Spectroscopy. CD-spectra were recorded on a Jasco J-715 spectropolarimeter (Tokyo, Japan) connected to a thermostat (Jasco PTC-348WI) with 1 mm quartz cells at 25 °C. Spectra were measured with a bandwidth of 1 nm, a sensitivity of 10 mdeg, and a response time of 2 s, with a scan speed of 50 $\text{nm}\cdot\text{min}^{-1}$, and were accumulated at least twice.

RESULTS

Binding of Oligoarginines onto Negatively Charged Lipid Vesicles: Kinetic Analysis. To investigate the kinetics of the peptide binding process to negatively charged POPC/POPG (3:7, molar ratio) vesicles, the fluorescence intensity of monomeric pyrene in pyrene-PG (RFI_M) was recorded as a function of time after addition of one of the peptides. Results are presented in Figures 1–3. The RFI_M -signal increases with time as a result of the peptide-vesicle association. Peptide **3** (polyarginine, Figure 1) induces the strongest signal response of all oligoarginines. The octaarginines (peptides **2**, **5**, and **7**, Figure 3) lead to a stronger fluorescence increase, as compared to the hexaarginines (peptides **1**, **4**, and **6**, Figure 2). On the basis of a mathematical fit of the experimental curves, it was found for all peptides that the fluorescence increase was biphasic with a fast first phase and a slow second phase (Figures 1–3). In general, higher peptide concentrations lead to a stronger fluorescence increase. Under conditions of maximal fluorescence increase (saturation response), the increase was analyzed by applying eq 1 which contains two exponential terms. From this analysis, the half-times ($t_{1/2}$) of the two phases can be obtained. The fast initial phase with $t_{1/2-1} = 2\text{--}5$ s is followed by the slower second phase with $t_{1/2-2} = 16\text{--}150$ s (Table 1). In the case of

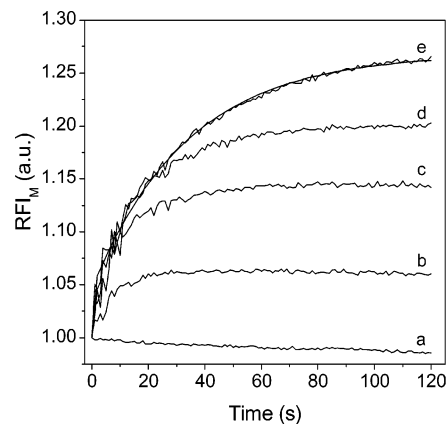


FIGURE 1: Binding kinetics of polyarginine **3** onto 100 nm POPC/POPG (3:7, molar ratio) LUVs monitored by the change of pyrene monomer fluorescence (RFI_M) in pyrene-PG. The final concentration of **3** was (a) 0 μM , (b) 0.05 μM , (c) 0.08 μM , (d) 0.12 μM , and (e) 0.42 μM . The total lipid concentration was 10 μM in 5 mM HEPES, 0.1 mM EDTA, and 150 mM NaCl, pH 7.4. Presented curves are mean curves of at least three measurements. The theoretical solid curve shown for curve e corresponds to a fit with eq 1 combining two exponential terms.

polyarginine, it was not possible to give a precise value for this peptide, as $t_{1/2-1}$ was below 2 s and beyond the limit of the measurement resolution. Clearly, the kinetics of the first phase is of the same order of magnitude for all oligoarginines ($t_{1/2-1} = 3\text{--}5$ s); however, the kinetics of the second phases differ significantly. A minimal half-time is obtained for peptide **4** ($\text{H}-(\beta\text{Arg})_6\text{-OH}$, $t_{1/2-2} = 16 \pm 3$ s), and a maximal half-time for peptide **7** ($\text{H}-(\beta\text{Arg})_8\text{-NH}_2$, $t_{1/2-2} = 150 \pm 21$ s). Furthermore the β -oligoarginine amides **6** and **7** show higher second half-times than the β -oligoarginine acids **4** and **5** of the same chain length.

Analysis of the Peptide Binding with the Complex Formation Model and Calculation of the Effective Peptide Charge. To investigate the thermodynamic binding parameters of the different peptides to the anionic vesicles, the fluorescence increase (ΔRFI_M) was plotted against the peptide concentration and analyzed with the complex formation model (Figure 4). From this model, the apparent binding constant ($K_{\text{app}1}$, see Materials and Methods) and the number of POPG lipids (n) bound to one peptide can be obtained. The determined binding constants are given in Table 2. The results show that, while the binding constants are of the same order of magnitude for the short oligoarginines **1**, **2**, and **4–7** (5.0×10^6 to $1.1 \times 10^7 \text{ M}^{-1}$), peptide **3**, with ~ 56 arginine residues, was found to have a binding constant of $1.8 \times 10^8 \text{ M}^{-1}$, which is larger by a factor of ~ 10 than the constants obtained for **1**, **2**, and **4–7**. The stronger binding of **3** is also reflected in the free energy of binding (ΔG°) that is $\sim 1.7\text{--}2.1 \text{ kcal mol}^{-1}$ lower than the ΔG° -values of the shorter oligoarginines (Table 2). The oligoarginines studied differ strongly in their n -values, ranging from 3.7 for peptide **4** up to 24.8 for peptide **3**. Furthermore, the β -oligoarginine amides **6** and **7** possess higher n -values than the β -oligoarginine acids **4** and **5** of the same chain length ($\Delta n \cong 4$). Also, the experimentally determined n -values of the α -oligoarginine acids **1** and **2** are higher than the n -values of the corresponding β -oligoarginine acids **4** and **5** ($\Delta n \cong 3\text{--}4$). This suggests that α - and β -oligoarginines containing the same number of guanidinium groups interact differently with anionic vesicles.

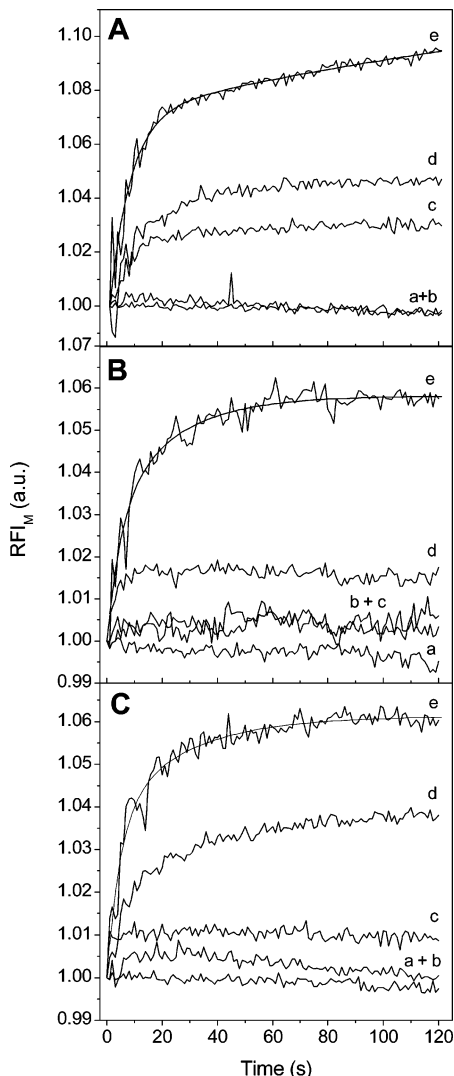


FIGURE 2: Binding kinetics of (A) H-(β Arg) $_6$ -NH $_2$ (**6**), (B) H-(β Arg) $_6$ -OH (**4**), and (C) H-(Arg) $_6$ -OH (**1**) onto 100 nm POPC/POPG (3:7, molar ratio) LUVs monitored by the change of pyrene monomer fluorescence (RFI $_M$) in pyrene-PG. The final concentrations of the added peptides were (a) 0 μ M, (b) 0.1 μ M, (c) 0.24 μ M, (d) 0.5 μ M, and (e) 4 μ M. The total lipid concentration was 10 μ M in 5 mM HEPES, 0.1 mM EDTA, and 150 mM NaCl, pH 7.4. Presented curves are mean curves of at least three measurements. The theoretical solid curve shown for curve e corresponds to a fit with eq 1 combining two exponential terms.

The determined values for the effective peptide charge (z_p) sensed at the membrane surface are presented in Table 2. It was found that all z_p -values are smaller than the corresponding number of POPG lipids (n) bound to one peptide and also smaller than the formal peptide charges (z_f). In this context, polyarginine (**3**) displays the greatest difference in z_p - and z_f -values. The calculated z_p of the β -oligoarginine amides **6** and **7** are higher than the z_p -values of the corresponding β -oligoarginines **4** and **5** possessing a C-terminal acid ($\Delta z_p \cong 2.5$ –3.5). Furthermore, the α -oligoarginine acids **1** and **2** have higher z_p -values than the β -oligoarginine acids **4** and **5** of the same chain length ($\Delta z_p \cong 2$ –3).

Analysis of the Vesicle Bilayer Fluidity and Permeability Changes upon Binding of the Peptides. When the relative fluorescence intensity of the excimer and monomer, that is, the RFI $_E$ /RFI $_M$ -ratio of the pyrene fluorescence in pyrene-

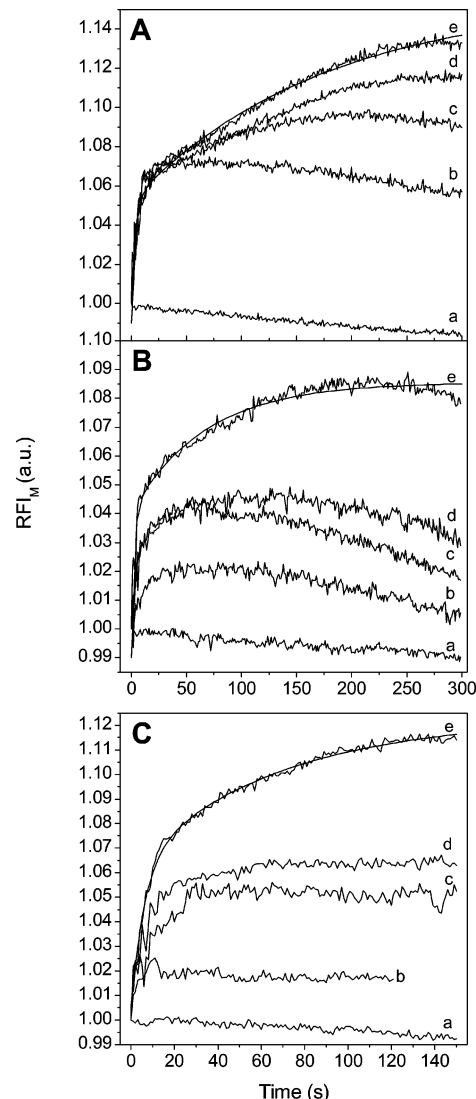


FIGURE 3: Binding kinetics of (A) H-(β Arg) $_8$ -NH $_2$ (**7**), (B) H-(β Arg) $_8$ -OH (**5**), and (C) H-(Arg) $_8$ -OH (**2**) onto 100 nm POPC/POPG (3:7, molar ratio) LUVs monitored by the change of pyrene monomer fluorescence (RFI $_M$) in pyrene-PG. The final concentrations of the added peptides were (a) 0 μ M, (b) 0.1 μ M, (c) 0.24 μ M, (d) 0.5 μ M, and (e) 4 μ M. The total lipid concentration was 10 μ M in 5 mM HEPES, 0.1 mM EDTA, and 150 mM NaCl, pH 7.4. Presented curves are mean curves of at least three measurements. The theoretical solid curve shown for curve e corresponds to a fit with eq 1 combining two exponential terms.

Table 1: Kinetic Parameters for the Binding of the Different Oligoarginines to 100 nm POPC/POPG (3:7, molar ratio) LUVs in 5 mM HEPES, 0.1 mM EDTA, and 150 mM NaCl, pH 7.4, 25 $^{\circ}$ C

compound	$t_{1/2-1^a}$ (s)	$t_{1/2-2}$ (s)
polyarginine (3)	<2	21 \pm 3
H-(β Arg) $_8$ -NH $_2$ (7)	3.0 \pm 0.5	150 \pm 21
H-(β Arg) $_8$ -OH (5)	3.0 \pm 0.4	64 \pm 13
H-(Arg) $_8$ -OH (2)	3.0 \pm 0.7	36 \pm 5
H-(β Arg) $_6$ -NH $_2$ (6)	5.0 \pm 0.8	52 \pm 28
H-(β Arg) $_6$ -OH (4)	5.0 \pm 2	16 \pm 3
H-(Arg) $_6$ -OH (1)	4.0 \pm 0.9	20 \pm 4

^a To obtain the kinetic parameters, the fluorescence increase (Figures 1–3) was fit to eq 1 containing two exponential terms (see Materials and Methods).

PG as a function of the peptide concentration is analyzed, it is possible to investigate the vesicle bilayer fluidity change

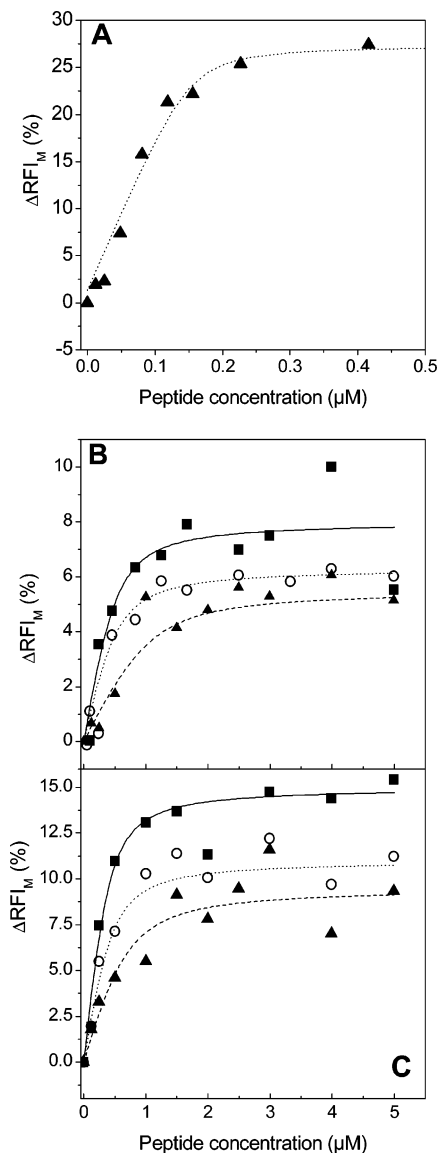


FIGURE 4: Concentration dependencies of the peptide binding onto 100 nm POPC/POPG (3:7, molar ratio) LUVs. (A) Polyarginine (3); (B) hexaarginines (■, H-(β Arg)₆-NH₂ (6); ▲, H-(β Arg)₆-OH (4); ○, H-(Arg)₆-OH (1)); (C) octaarginines (■, H-(β Arg)₈-NH₂ (7); ▲, H-(β Arg)₈-OH (5); ○, H-(Arg)₈-OH (2)). The total lipid concentration was 10 μ M in 5 mM HEPES, 0.1 mM EDTA, and 150 mM NaCl, pH 7.4. Each data point corresponds to three to five independent measurements with SD < 5.5% for polyarginine 3, SD < 2.5% for the octaarginines, and with SD < 2% for the hexaarginines. The solid, dotted, and dashed lines correspond to the theoretical binding curves that were obtained according to the complex formation model (see Materials and Methods).

induced by the addition of the peptides. A decreased RFI_E/RFI_M of symmetrically labeled vesicles (outer and inner leaflet) is usually attributed to a decreased mobility of the pyrene-PG lipids within the lipid bilayer (smaller lipid lateral diffusion coefficient resulting in less excimers formed by collisions). This corresponds to a rigidification of the lipid bilayer. All peptides decrease the RFI_E/RFI_M-ratio significantly, suggesting that vesicle-bound peptides reduce the lateral diffusion of the lipids in the membrane (Figure 5). Mean values for $\Delta(\text{RFI}_E/\text{RFI}_M)$ observed after the saturation response are given in Table 3. The $\Delta(\text{RFI}_E/\text{RFI}_M)$ -values vary between $-12 \pm 2\%$ for H-(β Arg)₆-OH (4) and $-35 \pm 1.5\%$ for polyarginine (3). The octaarginines 2, 5, and 7 induce a

Table 2: Thermodynamic Parameters for the Binding of the Different Oligoarginines to 100 nm POPC/POPG (3:7, molar ratio) LUVs in 5 mM HEPES, 0.1 mM EDTA, and 150 mM NaCl, pH 7.4, 25 °C

compound	K_{app1}^a (M ⁻¹)	n^a	z_p^b	z_f^c	ΔG° (kcal mol ⁻¹) ^d
polyarginine (3)	1.8×10^8	24.8	14.1–18.0	~56	-11.27
H-(β Arg) ₈ -NH ₂ (7)	1.1×10^7	10	5.7–7.0	9	-9.61
H-(β Arg) ₈ -OH (5)	5.6×10^6	6	3.4–4.2	9	-9.20
H-(Arg) ₈ -OH (2)	8.9×10^6	9	5.7–7.0	9	-9.47
H-(β Arg) ₆ -NH ₂ (6)	8.9×10^6	7.8	4.5–5.5	7	-9.47
H-(β Arg) ₆ -OH (4)	5.0×10^6	3.7	2.3–3.0	7	-9.13
H-(Arg) ₆ -OH (1)	7.8×10^6	7.9	4.5–5.5	7	-9.39

^a Obtained from the complex formation model, which assumes that the peptides (P) bind independently to n POPG lipids (L): $P + L_n = P \times L_n$. K_{app1} represents the binding constant for the binding of the peptides to peptide-free vesicles. ^b Calculated effective peptide charge (z_p) required to reduce the charge of the negatively charged vesicles at saturation by 80–100%. ^c Formal peptide charge (equals number of Arg-residues + positively charged N-terminus). ^d Obtained according to $\Delta G^\circ = -RT \ln K_{\text{app1}}$.

stronger decrease of the RFI_E/RFI_M-ratio than the hexaarginines 1, 4, and 6: -20 to -25% (octaarginines) versus -12 to -18% (hexaarginines). This indicates that the octaarginines more strongly rigidify the membrane bilayer than the hexaarginines do. In line with this finding, polyarginine (3) clearly leads to the strongest bilayer rigidification ($\Delta(\text{RFI}_E/\text{RFI}_M)$: $-35 \pm 1.5\%$).

To investigate the permeability change of the anionic vesicle bilayer, calcein was entrapped inside the anionic vesicles and the release measured upon addition of the peptides (Figure 6, Table 3). The addition of the hexaarginines 1, 4, and 6 to the vesicles did not induce a significant leakage. In contrast, the octaarginines 2, 5, and 7 increased the permeability of the vesicle bilayer toward calcein (leakage $\cong 13$ –27% after 1200 s). Among the series of octaarginines tested, 7 (H-(β Arg)₈-NH₂) was found to induce a calcein release approximately twice that determined for 2 and 5 (H-(Arg)₈-OH and H-(β Arg)₈-OH) (Table 3). Polyarginine (3) induced the strongest measured leakage of all peptides ($\sim 60\%$ after 1200 s).

Comparison of the Peptide–Vesicle Binding Kinetics with the Calcein Release Kinetics. We found sigmoidal calcein release kinetics from the anionic vesicles (insets of Figure 7A,C). Aiming at better understanding the relationship between the binding- and leakage kinetics, we compared the two time progresses for the peptides that showed the strongest interaction with the anionic lipid bilayer (i.e., 3 and 7). Within the initial phase of binding ($t_{1/2-1} \cong < 2$ –5 s) there is no peptide-induced leakage. In the following second phase of binding ($t_{1/2-2}$, see Table 1), the leakage increased up to $\sim 15\%$ for 7 (after 300 s) and up to $\sim 30\%$ for 3 (after 120 s). This observation indicates that binding of the peptide directly induces calcein release from the vesicles. The RFI_M-signal reached equilibrium, and calcein is slowly and continuously released from the vesicles (slow increase of the leakage kinetic curves).

Structural Analysis of Vesicle-Bound H-(β Arg)₈-NH₂ with CD Spectroscopy. Since peptide 7 promoted the strongest leakage of all tested hexa- and octaarginines, possible conformational changes of the peptide upon binding to the vesicles were studied by CD. H-(β Arg)₈-NH₂ (7) adopts a helical secondary structure, an (M)-3₁₄-helix, in methanol

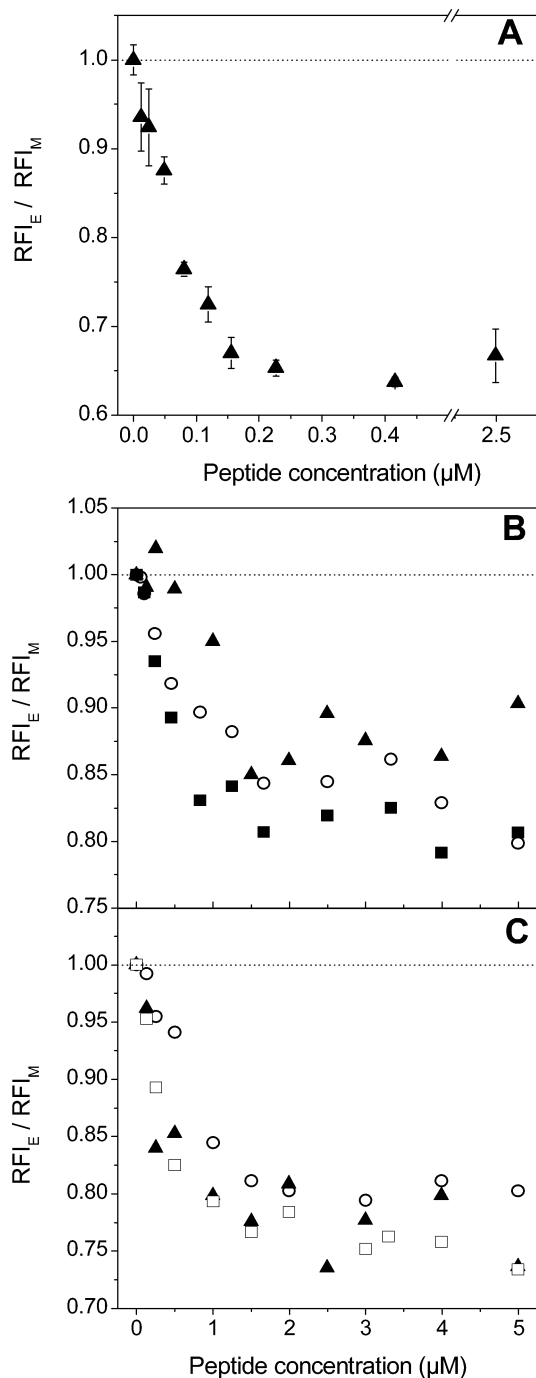


FIGURE 5: Effect of the peptide concentration on the excimer-to-monomer ratio RFI_E/RFI_M of pyrene fluorescence in pyrene-PG. The peptides were added to 100 nm POPC/POPG (3:7, molar ratio) LUVs. (A) Polyarginine (3); (B) hexaarginines (■, H-(β Arg) $_6$ -NH $_2$ (6); ▲, H-(β Arg) $_6$ -OH (4); ○, H-(Arg) $_6$ -OH (4)); (C) octaarginines (□, H-(β Arg) $_8$ -NH $_2$ (7); ▲, H-(β Arg) $_8$ -OH (5); ○, H-(Arg) $_8$ -OH (2)). The total lipid concentration was 10 μ M in 5 mM HEPES, 0.1 mM EDTA, and 150 mM NaCl, pH 7.4. Each data point corresponds to three to five independent measurements with SD < 0.04 for polyarginine 3, SD < 0.04 for the octaarginines (2, 5, 7), and with SD < 0.02 for the hexaarginines (1, 4, 6).

(44, 45). A negative Cotton effect near 215 nm and a 0-passage at \sim 207 nm in the CD-spectrum are characteristic of this kind of helical structure (Figure 8). The CD-spectra give no indication that H-(β Arg) $_8$ -NH $_2$ (7) adopts a helical conformation in buffer, or in the presence of anionic vesicles (POPC/POPG = 3:7, molar ratio). The tested molar lipid-to-peptide ratios ($[L]_{tot}/[P]_{tot}$) were 2.5/1 and 10/1 (Figure

Table 3: Influence of the Vesicle Binding of the Different Oligoarginines on the Bilayer Fluidity and Permeability: LUVs, POPC/POPG (3:7, molar ratio), 5 mM HEPES, 0.1 mM EDTA, and 150 mM NaCl, pH 7.4, 25 $^{\circ}$ C

compound	$\Delta(RFI_E/RFI_M)$ (%) ^a	leakage (%) ^b
polyarginine (3)	-35 ± 1.5	60.0
H-(β Arg) $_8$ -NH $_2$ (7)	-25 ± 1.5	26.6 ± 5.1
H-(β Arg) $_8$ -OH (5)	-23 ± 3	13.3 ± 2.6
H-(Arg) $_8$ -OH (2)	-20 ± 1	17.3 ± 1.6
H-(β Arg) $_6$ -NH $_2$ (6)	-18 ± 1.5	3.0
H-(β Arg) $_6$ -OH (4)	-12 ± 2	0
H-(Arg) $_6$ -OH (1)	-16 ± 2	0.3

^a Mean relative decrease of the RFI_E/RFI_M -ratio at saturation.

^b Calcein release determined for peptide concentrations at saturation (2–5 μ M).

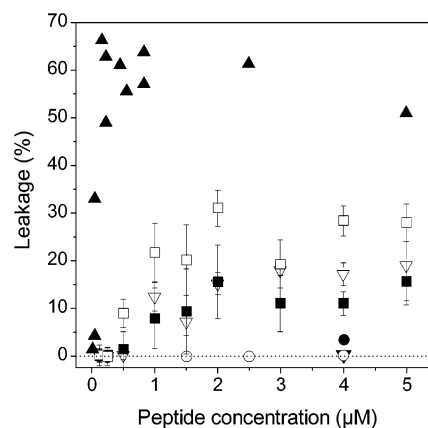


FIGURE 6: Calcein release from 100 nm POPC/POPG (3:7, molar ratio) LUVs as a function of the peptide concentration (▲, polyarginine (3); □, H-(β Arg) $_8$ -NH $_2$ (7); ■, H-(β Arg) $_8$ -OH (5); ▽, H-(Arg) $_8$ -OH (2); ●, H-(β Arg) $_6$ -NH $_2$ (6); ○, H-(β Arg) $_6$ -OH (4); ▼, H-(Arg) $_6$ -OH (1)). The presented leakage values were obtained after 1200 s incubation with the peptides. The total lipid concentration was 10 μ M in 5 mM HEPES, 0.1 mM EDTA, and 150 mM NaCl, pH 7.4.

8). Higher $[L]_{tot}/[P]_{tot}$ -ratios could not be analyzed, as the vesicle suspensions became too turbid.

DISCUSSION

In the present study, we have investigated the interaction of α - and β -oligoarginine acids and amides and of polyarginine (Scheme 1, 1–7), with anionic lipid vesicles composed of POPC and POPG at pH 7.4. The goal was to compare the thermodynamic and kinetic parameters for the interaction of these cationic peptides with negatively charged membrane bilayers. At present, we are not aware of any reports that compare such oligoarginines with respect to vesicle binding. In addition, the unusual properties of β -oligoarginines, such as their stability against peptidases, their outstanding metabolic stability, and lack of antibiotic activity, make them of interest with respect to vesicle binding and permeation (46–48). With respect to the biological activity of oligoarginines as CPPs, the formation of complexes between the positively charged guanidinium groups and negatively charged groups on the cell surface, such as membrane PG-lipids and heparan sulfate proteoglycans (23), is most likely an important initial step for transport across the hydrophobic barrier of a lipid bilayer.

Binding and Leakage Kinetics. Binding kinetics of all oligoarginines are biphasic (Figures 1–3, Table 1). The

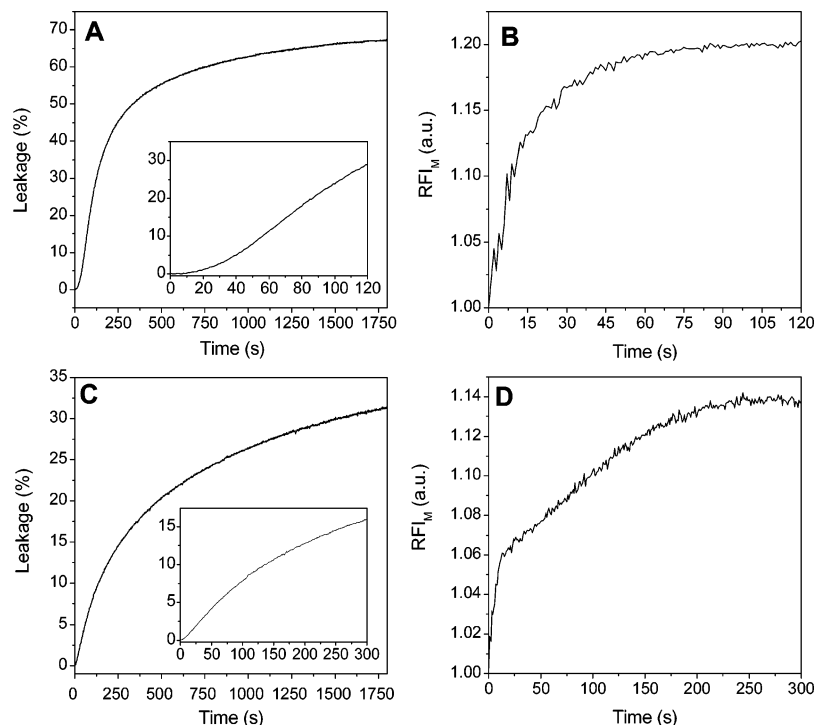


FIGURE 7: Comparison of the calcein release kinetics from 100 nm POPC/POPG (3:7, molar ratio) LUVs with the corresponding peptide binding kinetics. (A) Calcein release kinetics after addition of 0.12 μM polyarginine (**3**) and (B) the corresponding binding kinetics. (C) Calcein release kinetics after addition of 4 μM H-(βArg)₈-NH₂ (**7**) and (D) the corresponding binding kinetics. The total lipid concentration was 10 μM in 5 mM HEPES, 0.1 mM EDTA, and 150 mM NaCl, pH 7.4. The two insets in panels A and C represent zoom-ins.

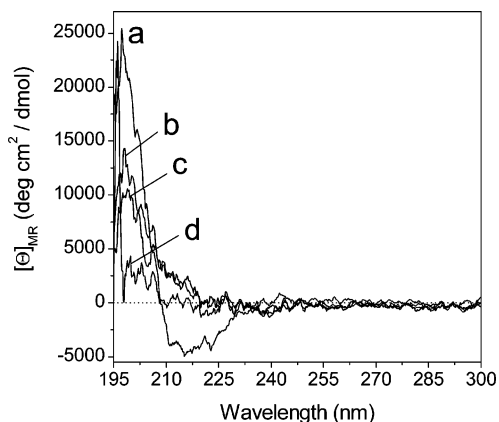


FIGURE 8: Normalized CD spectra of H-(βArg)₈-NH₂ (**7**). (a) 80 μM in methanol; (b) 80 μM in buffer (5 mM HEPES, 0.1 mM EDTA, and 150 mM NaCl, pH 7.4); (c) 80 μM in the presence of POPC/POPG (3:7, molar ratio) LUVs (200 μM total lipid concentration) in buffer; and (d) 50 μM in the presence of POPC/POPG (3:7, molar ratio) LUVs (500 μM total lipid concentration) in buffer. Plotted is the mean residue ellipticity $[\Theta]_{\text{MR}}$ as a function of the wavelength.

second binding step is 1 order of magnitude slower with respect to the first and is therefore rate-limiting. The corresponding leakage kinetics (especially for polyarginine **3** and peptide **7**) show sigmoidal initial time courses (Figure 7). During the first binding phase, no calcein is released from the vesicles, whereas during the second binding phase, calcein begins to leak out. This behavior suggests that the interaction of the cationic peptides with the anionic POPC/POPG (3:7, molar ratio) vesicles must reach a certain strength in order to disrupt the bilayer structure. From a mechanistic point of view, this indicates that during the first ~ 5 –10 s the peptides bind loosely to the anionic lipid bilayer. During

this time period, the bilayer structure remains mostly intact. Within the second binding phase (~ 40 –300 s), the peptides attach more strongly, the bilayer becomes rigidified (see Figure 5), and calcein is released. Sigmoidal leakage time courses were also observed by Matile and co-workers (49) when studying the interaction of polyarginine (molecular weight 14 000, degree of polymerization 72) with egg yolk POPC/egg yolk POPG (1/1) LUVs (49). On the other hand, in a study of the membrane destabilizing properties of arginine-rich CPPs with DOPC/DOPG (60:40) vesicles, Thorén et al. (50) did not find significant leakage, although membrane aggregation and fusion was induced by the tested peptides. These contradicting results lead to the conclusion that the chemical nature of the lipid and/or the mole fraction of anionic lipid determine the extent of leakage of aqueous content from dye-loaded vesicles. To further test this point, we investigated the interaction of oligoarginines with POPC/POPG (molar ratio = 7:3) lipid bilayers that are considerably less negatively charged than the vesicles composed of POPC/POPG at a molar ratio of 3:7. We found that cationic polyarginine **3** and peptide **7** bind to the vesicles and induce vesicle aggregation with no measurable release of calcein (data not shown). This finding suggests that a certain amount of negative charge on the vesicle surface is necessary to promote calcein-release from lipid-bilayers with associated oligoarginines. Interestingly, the two oligoarginine amides **6** and **7** have $t_{1/2-2}$ -values that are 2–3 times larger than the $t_{1/2-2}$ of the corresponding oligoarginine acids **4** and **5**. This finding leads us to conclude that the terminal amide group increases the interaction of the cationic peptides with the anionic vesicles. In comparison, the half-time of polyarginine **3** ($t_{1/2-2} = 21 \pm 3$ s) is rather short. This low value may have its origin in the higher number of positive charges

($z_f \sim 56$) possessed by polyarginine **3** with respect to the shorter oligoarginines ($z_f = 7-9$). This may lead to a faster overall association process. Biphasic time courses were also reported for the interaction of cationic annexins with anionic POPC/POPG vesicles and for the anionic assembly factor P17 (net charge of -7 at pH 7.2) with cationic vesicles composed of phosphatidylcholine, phosphatidylethanolamine, and sphingosine lipids (51, 52). In both cases, the bilayer association was completed after $\sim 250-500$ s.

In general, it is suggested that the binding of charged proteins to oppositely charged vesicle membranes is composed of at least two steps (53). The initial binding step is mainly driven by electrostatic interactions that result in an overall charge neutralization at the contact side. This binding step takes place near the interface and leads to a thinning of the membrane (Shai–Matsuzaki–Huang model) (54). The second step may also involve hydrophobic interactions and/or hydrogen bonding, including a significant disruption of the membrane. According to this premise, the first peptide binding phase reported herein most likely corresponds to electrostatic attraction that neutralizes the peptide charge near the interface, whereas the second binding phase also involves nonelectrostatic forces, which cause leakage of the bilayer. To further explore this possibility, we analyzed in more detail the energetic contributions of the binding event to the total free energy of binding.

Thermodynamic Analysis. Initial analysis revealed the binding constant (K_{app1}) of polyarginine **3** to be approximately 1 order of magnitude larger than the K_{app1} -values calculated for the oligoarginines, corresponding to a difference in the free energy of binding of ~ -1.7 to -2.1 kcal/mol (Table 2). Calculated K_{app1} values for the hexa- and octaarginines were shown to be of the same order of magnitude ($\sim 5 \times 10^6$ to 10^7 M $^{-1}$), indicating similar binding strengths for the anionic vesicles. A related study has recently been performed for the association of H-(Arg)₉OH with anionic POPC/POPG (7:3, molar ratio) vesicles; a binding constant of 8.2×10^4 M $^{-1}$ was reported (23). This is approximately 2 orders of magnitude lower than the binding constants reported herein for the association onto POPC/POPG (3:7, molar ratio) vesicles with the opposite lipid ratio. Similar observations have been made for the binding of heptalysine onto POPC/POPS vesicles. A reduction of POPS from 17% to 4% molar reduced the molar partitioning coefficient by a factor of ~ 1000 (55).

The stronger peptide-vesicle interaction of polyarginine (**3**) is also reflected in a higher number of bound POPG lipids per peptide (n) and in a higher effective peptide charge value (z_p) sensed at the membrane surface. This is reasonable, since this polyarginine possesses 7–10 times the number of guanidinium groups per peptide chain as compared to the oligoarginines **1**, **2**, and **4–7**. However, the determined n -value of polyarginine (**3**) is rather low (~ 25). As **3** has a formal charge (z_f) of $\sim +56$, this indicates that only about 45% of this charge is electrically neutralized with $n \cong 25$. A similar phenomenon was observed by Hartmann and Galla (56) for polylysine. Their investigation showed that only every second lysine-residue was bound to a lipid. The calculated z_p of **3** for complete charge neutralization at saturation is even lower ($z_p = 14-18$, Table 2). Lower effective peptide charge (z_p) with respect to the formal charge (z_f) has also recently been observed for the binding

Table 4: Nonelectrostatic and Electrostatic Contributions of the Different Oligoarginines to the Total Free Energy of Binding onto POPC/POPG (3:7, molar ratio) LUVs in 5 mM HEPES, 0.1 mM EDTA, and 150 mM NaCl, pH 7.4, 25 °C

compound	K_{app2} (M $^{-1}$) ^a	ΔG_{el} (kcal mol $^{-1}$) ^b	$\Delta G_{nonelect}$ (kcal mol $^{-1}$) ^c	%- ΔG_{el} ^d
polyarginine (3)	6.1×10^5	-3.38	-7.88	30
H-(β Arg) ₈ -NH ₂ (7)	8.9×10^4	-2.86	-6.75	30
H-(β Arg) ₈ -OH (5)	8.3×10^4	-2.49	-6.71	27
H-(Arg) ₈ -OH (2)	8.9×10^4	-2.73	-6.75	29
H-(β Arg) ₆ -NH ₂ (6)	1.0×10^5	-2.66	-6.82	28
H-(β Arg) ₆ -OH (4)	1.0×10^5	-2.28	-6.85	25
H-(Arg) ₆ -OH (1)	9.4×10^4	-2.61	-6.78	27

^a Calculated according to $K_p = K_{app2} = X_b/[P]$. [P] is the bulk equilibrium concentration. K_{app2} was calculated at saturation, where the concentration directly above the bilayer surface is approximately equal to the bulk equilibrium concentration [P]. ^b The electrostatic free energy of the peptide binding (ΔG_{el}) was calculated according to $-RT \ln(K_{app1}/K_{app2})$. ^c The nonelectrostatic contribution ($\Delta G_{nonelect}$) can be obtained according to $-RT \ln K_{app2}$. ^d %- $\Delta G_{el} = (\Delta G_{el}/(\Delta G_{el} + \Delta G_{nonelect})) \times 100$.

of H-(Arg)₉-OH onto POPC/POPG (7:3) vesicles and for other CPPs (23, 42, 57). It is argued that this phenomenon reflects the polyelectrolytic behavior of such cationic peptides. In buffer, such components will attract counterions that will not be fully released when peptide-vesicle association occurs. Accordingly, we find for all oligoarginines that $z_p < z_f$ (Table 2). Interestingly, the difference between z_p and z_f is larger for the investigated β -oligoarginine acids **4** and **5** ($z_p/z_f \cong 0.45$) than for α -oligoarginine acids **1** and **2** ($z_p/z_f \cong 0.78$). This finding suggests that either β -oligoarginines more strongly attract counterions from the aqueous surrounding and/or α -oligoarginines better expose their positive charges to the vesicles. This would also explain the higher number of bound lipids per peptide observed for α -oligoarginines (see Table 2).

Strong differences concerning the n - and z_p -values were also observed between β -oligoarginine acids and amides (Table 2). The β -oligoarginine amides **6** and **7** possess larger n - and z_p -values than the corresponding acids, **4** and **5**. This observation indicates that the terminal amide group interacts with the membrane surface and/or that the acid group reduces the number of bound lipids due to charge repulsion with phosphate-anions of POPG. In terms of the hydrogen-bonding properties of amides, the additional interaction by the amide group may involve hydrogen bonding near the interface at the membrane hydration layer.

To distinguish electrostatic from nonelectrostatic energetic contributions to the total free energy of binding (ΔG°), we calculated K_{app2} at the saturation response for all peptides (Table 4). The determined K_{app2} -values (8.3×10^4 to 6.1×10^5 M $^{-1}$) are about 2 orders of magnitude smaller than the K_{app1} -values, the binding constants describing the association onto peptide-free vesicles. Assuming that the surface potential is reduced to zero when reaching saturation response, K_{app2} represents the binding constant onto a neutral vesicle and hence the *nonelectrostatic* energetic contribution: $\Delta G_{nonelect} = -RT \ln K_{app2}$. The *electrostatic* contribution to the free energy of binding can therefore be estimated by the following equation: $\Delta G_{el} = -RT \ln(K_{app1}/K_{app2})$ (38). Data for the energetic contributions are given in Table 4. Analysis reveals that only about 25–30% of the total free energy of binding has electrostatic origin. A similar value has also recently been reported for H-(Arg)₉-OH binding onto POPC/POPG vesicles

(23). The authors calculated a $\%-\Delta G_{el}$ of 33% for a peptide concentration of 1 μM . In contrast, studies investigating the binding of cell-penetrating peptide H-(Arg)₇Trp-OH onto DOPC/DOPG vesicles reported electrostatic contributions of more than 50% (57). Strong nonelectrostatic contributions can be explained by the hydrogen-bonding properties of the bivalent guanidinium group of arginine that allows strong interaction with the membrane hydration layer, which extends 1–3 nm into the aqueous phase (23). On the other hand, high nonelectrostatic contributions are also indicative of a transfer from the aqueous phase into the less polar environment of the lipid bilayer (58).

Analysis of Vesicle Bilayer Destabilization. The investigated oligoarginines decrease the $\text{RFI}_E/\text{RFI}_M$ -ratio of pyrene fluorescence in pyrene-PG in the following order: **3** (~56 Arg residues) > **2, 5, 7** (eight Arg residues) > **1, 4, 6** (six Arg residues). Since the vesicles are labeled symmetrically, it is unlikely that the signal change arises from a flip-flop mechanism of the POPG lipids. It is more likely that the adsorbed peptides decrease the lateral mobility of the phospholipids. Such observations have also been reported for other basic peptides and proteins such as polylysine, cytochrome *b*₅, histones, and H-(Lys)₁₉-OH (27, 55, 59). Domain formation of negatively charged POPG lipids would require an increased $\text{RFI}_E/\text{RFI}_M$ -ratio, a phenomenon that was not observed in the present study. The membrane rigidification is directly correlated to the determined leakage (Table 3): **3** > **7** > **2** \geq **5** \gg **1, 4, 6**. None of the hexaarginines induce significant calcein release, although their K_{app} -values are of the same order of magnitude as those of the octaarginines. It is likely that the somewhat stronger membrane rigidification induced by the octaarginines is necessary to induce leakage of the anionic vesicles, possibly by promoting a positive curvature (60). Interestingly, the calcein release data obtained for **6** and **7** correlate well with the cell-uptake efficiency determined for corresponding fluorescein-labeled derivatives (14): increased calcein release corresponds to a more efficient cell uptake. Also of importance is that β -peptide **7**, which possesses a C-terminal amide group, induces approximately twice as much calcein release as β -peptide **5** with C-terminal acid group. This finding suggests that the ability of the amide-form of the β -peptide **7** to interact with more POPG lipids than the acid form **5** (see Table 2) leads to a stronger membrane disruption, and therefore, more calcein is released from the vesicles.

Analysis of Peptide Structure. Recent studies have shown that cationic β -peptides containing cyclic amino acid residues are potent bilayer-disrupting agents and that 14-helix formation in the presence of anionic vesicles is necessary for bilayer disruption (61). However, our CD analysis of oligoarginine **7** (H-(β Arg)₈-NH₂) in the presence of anionic POPC/POPG vesicles shows that the formation of a 14-helix conformation is not required for membrane permeabilization (Figure 8). Similar observations have recently been reported for the cell-penetrating α -peptide H-(Arg)₇Trp-OH, which was also shown not to adopt an ordered structure in the presence of anionic vesicles for an $[\text{L}]_{tot}/[\text{P}]_{tot}$ of 100:1 (57).

Another interesting aspect of our investigations relates to the observed *nonendocytotic* uptake of oligoarginines into live cells (15, 20, 21). Our binding studies show that, if the interaction is strong enough ($K_{app} \cong 10^5\text{--}10^6 \text{ M}^{-1}$, significant membrane rigidification), LUVs with a mean diameter of

100 nm become permeable. For polyarginine, efficient leakage (~60%, Figures 6 and 7) is already observed at a $[\text{L}]_{tot}/[\text{P}]_{tot}$ -ratio of ~100 and matches the $[\text{L}]_{tot}/[\text{P}]_{tot}$ -ratios of known pore-forming peptides (62). Also, the octaarginine amide **7** induces significant leakage of ~20% at a $[\text{L}]_{tot}/[\text{P}]_{tot}$ -ratio of 10. As mentioned previously, the interaction of oligoarginines with cell surface GAGs such as heparan sulfate is most likely necessary in order to observe efficient internalization. A possible explanation is the very high affinity that oligoarginines, such as H-(Arg)₉-OH, show toward heparan sulfate. In recent studies, association constants in the range of $\sim 10^6 \text{ M}^{-1}$ were determined for the binding to heparin and heparan sulfate. This is in agreement with the binding constants obtained in this study for the binding of oligoarginines onto strongly negatively charged vesicles (POPC/POPG = 3:7, molar ratio). Such strong binding may lead to significant membrane disruption allowing arginine-rich CPPs to cross the vesicle bilayer in a nonendocytotic manner. Also, the escape from endocytotic vesicles requires the membrane bilayer to become permeable, thereby permitting the CPP to enter into the cytoplasm of the cell (3, 24).

Although it was not the focus of the present work, the thermodynamics of binding of the amino cationic polylysine to anionic POPC/POPG vesicles (7:3, molar ratio) containing pyrene-PG was compared with the binding of the guanidinium cationic polyarginine **3** (see Supporting Information). Although both polypeptides had a similar degree of polymerization, **3** led to a stronger increase of the monomer pyrene fluorescence (ΔRFI_M) than polylysine (see Figure S-2, Supporting Information). Furthermore, a preliminary analysis with the complex formation model showed that K_{app1} is about three times larger than K_{app1} for polylysine, and **3** binds to twice as many POPG molecules than polylysine.

CONCLUSIONS

We have shown, for a range of α - and β -oligoarginines (see Scheme 1) with C-terminal amide and acid end-groups, clear differences in their interaction with anionic lipid vesicles (POPC/POPG = 3:7, molar ratio): (i) polyarginine (**3**) binds with an association constant approximately 1 order of magnitude higher than those of the shorter oligoarginines **1, 2, and 4–7**, and polyarginine (**3**), leads to the strongest bilayer rigidification and induces the largest membrane disruption (leakage); (ii) all octaarginines (peptides **2, 5, and 7**) induce significant vesicle leakage (13–30%), whereas hexaarginines (peptides **1, 4, and 6**) do not; (iii) β -oligoarginine amides (peptides **6** and **7**) interact with more lipids and induce a stronger bilayer disruption than the corresponding acids (peptides **4** and **5**); and (iv) α -oligoarginine acids (peptides **1** and **2**) interact with more lipids and expose a higher effective peptide charge to the anionic vesicles than the corresponding β -oligoarginine acids (peptides **4** and **5**).

We calculate that for all oligoarginines significantly less than 50% of the total free energy of binding has electrostatic origin. Such observations are supported by the finding that the stronger vesicle association of polyarginine with respect to the oligoarginines has nonelectrostatic origins. Kinetic analysis of the binding processes shows biphasic time courses. We suggest that the first fast process (4–10 s) corresponds to weaker electrostatic attraction, whereas the

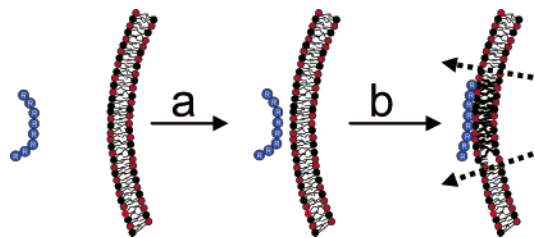


FIGURE 9: Proposed mechanism for the binding of oligoarginines onto anionic POPC/POPG vesicles. (a) *Initial electrostatic interaction* that is fast, nonspecific, and relatively weak ($-\Delta G_{el} \sim 25\text{--}30\%$ of the total free energy of binding) followed by (b) *nonelectrostatic interaction* that is rate-limiting and stronger ($-\Delta G_{nonel} \sim 70\text{--}75\%$ of the total free energy of binding) and leads to bilayer rigidification and disruption allowing release of aqueous content from inside the vesicle (shown as dotted arrows).

second slower binding step (32–300 s) involves stronger nonelectrostatic forces and membrane disruption (for a schematic presentation of the binding events, see Figure 9). Such observations are relevant to (i) the general question of how arginine-rich CPPs may enter the cell via a nonendocytotic mechanism and (ii) how arginine-rich CPPs may escape from endocytotic vesicles into the cytosol.

ACKNOWLEDGMENT

We are grateful to Prof. Heidi Wunderli-Allenspach and Prof. François Diederich (Department of Chemistry and Applied Biosciences) for allowing us to use their DLS and CD equipment, respectively. We thank Dr. Martin Müller (Department of Physics) for the cryo-TEM analysis.

SUPPORTING INFORMATION AVAILABLE

A detailed description of the synthesis of peptides, formulas used for the fitting of the experimental data for K_{app1} and n , equations related to the counterion binding and to the determination of K_{app2} , and experimental data for the binding of polylysine to anionic vesicles. This material is available free of charge via the Internet at <http://pubs.acs.org>.

REFERENCES

- Trehin, R., and Merkle, H. P. (2004) Chances and pitfalls of cell penetrating peptides for cellular drug delivery, *Eur. J. Pharm. Biopharm.* 58, 209–223.
- Lochmann, D., Jauk, E., and Zimmer, A. (2004) Drug delivery of oligonucleotides by peptides, *Eur. J. Pharm. Biopharm.* 58, 237–251.
- Fischer, R., Fotin-Mleczek, M., Hufnagel, H., and Brock, R. (2005) Break on through to the other side—biophysics and cell biology shed light on cell-penetrating peptides. *ChemBioChem* 6, 2126–2142.
- Astriab-Fisher, A., Sergueev, D., Fisher, M., Shaw, B. R., and Juliano, R. L. (2002) Conjugates of antisense oligonucleotides with the Tat and antennapedia cell-penetrating peptides: Effects on cellular uptake, binding to target sequences, and biologic actions, *Pharm. Res.* 19, 744–754.
- Schwarze, S. R., Ho, A., Vocero-Akbani, A., and Dowdy, S. F. (1999) In vivo protein transduction: Delivery of a biologically active protein into the mouse, *Science* 285, 1569–1572.
- Muratovska, A., and Eccles, M. R. (2004) Conjugate for efficient delivery of short interfering RNA (siRNA) into mammalian cells, *FEBS Lett.* 558, 63–68.
- Torchilin, V. P., and Levchenko, T. S. (2003) TAT-liposomes: A novel intracellular drug carrier, *Curr. Protein Pept. Sci.* 4, 133–140.
- Vives, E., Brodin, P., and Lebleu, B. (1997) A truncated HIV-1 Tat protein basic domain rapidly translocates through the plasma membrane and accumulates in the cell nucleus, *J. Biol. Chem.* 272, 6010–6017.
- Derossi, D., Joliot, A. H., Chassing, G., and Prochiantz, A. (1994) The 3rd helix of the antennapedia homeodomain translocates through biological-membranes, *J. Biol. Chem.* 269, 10444–10450.
- Wender, P. A., Mitchell, D. J., Pattabiraman, K., Pelkey, E. T., Steinman, L., and Rothbard, J. B. (2000) The design, synthesis, and evaluation of molecules that enable or enhance cellular uptake: Peptoid molecular transporters *Proc. Natl. Acad. Sci. U.S.A.* 97, 13003–13008.
- Mitchell, D. J., Kim, D. T., Steinman, L., Fathman, C. G., and Rothbard, J. B. (2000) Polyarginine enters cells more efficiently than other polycationic homopolymers *J. Pept. Res.* 56, 318–325.
- Wright, L. R., Rothbard, J. B., and Wender, P. A. (2003) Guanidinium rich peptide transporters and drug delivery, *Curr. Protein Pept. Sci.* 4, 105–124.
- Rueping, M., Mahajan, Y., Sauer, M., and Seebach, D. (2002) Cellular uptake studies with β -peptides, *ChemBioChem* 3, 257–259.
- Seebach, D., Namoto, K., Mahajan, Y. R., Bindschadler, P., Sustmann, R., Kirsch, M., Ryder, N. S., Weiss, M., Sauer, M., Roth, C., Werner, S., Beer, H. D., Munding, C., Walde, P., and Voser, M. (2004) Chemical and biological investigations of β -oligoarginines, *Chem. Biodiversity* 1, 65–97.
- Geueke, B., Namoto, K., Agarkova, I., Perriard, J. C., Kohler, H. P. E., and Seebach, D. (2005) Bacterial cell penetration by β^3 -oligohomoarginines: Indications for passive transfer through the lipid bilayer, *ChemBioChem* 6, 982–985.
- Potocky, T. B., Menon, A. K., and Gellman, S. H. (2003) Cytoplasmic and nuclear delivery of a TAT-derived peptide and a β -peptide after endocytic uptake into HeLa cells, *J. Biol. Chem.* 278, 50188–50194.
- Luedtke, N. W., Carmichael, P., and Tor, Y. (2003) Cellular uptake of aminoglycosides, guanidinoglycosides, and poly-arginine, *J. Am. Chem. Soc.* 125, 12374–12375.
- Futaki, S., Nakase, I., Suzuki, T., Zhang, Y. J., and Sugiura, Y. (2002) Translocation of branched-chain arginine peptides through cell membranes: Flexibility in the spatial disposition of positive charges in membrane-permeable peptides, *Biochemistry* 41, 7925–7930.
- Futaki, S., Goto, S., Suzuki, T., Nakase, I., and Sugiura, Y. (2003) Structural variety of membrane permeable peptides, *Curr. Protein Pept. Sci.* 4, 87–96.
- Thorén, P. E., Persson, D., Isakson, P., Goksör, M., Önfelt, A., and Nordén, B. (2003) Uptake of analogs of penetratin, Tat(48–60) and oligoarginine in live cells, *Biochem. Biophys. Res. Commun.* 307, 100–107.
- Zaro, J. L., and Shen, W. C. (2005) Evidence that membrane transduction of oligoarginine does not require vesicle formation, *Exp. Cell Res.* 307, 164–173.
- Rothbard, J. B., Jessop, T. C., Lewis, R. S., Murray, B. A., and Wender, P. A. (2004) Role of membrane potential and hydrogen bonding in the mechanism of translocation of guanidinium-rich peptides into cells, *J. Am. Chem. Soc.* 126, 9506–9507.
- Gonçalves, E., Kitas, E., and Seelig, J. (2005) Binding of oligoarginine to membrane lipids and heparan sulfate: structural and thermodynamic characterization of a cell-penetrating peptide. *Biochemistry* 44, 2692–2702.
- Fuchs, S. M., and Raines, R. T. (2004) Pathway for polyarginine entry into mammalian cells, *Biochemistry* 43, 2438–2444.
- Yuhong, Xu., Sek-Wen, Hui., Frederik, P., and Szoka, F. C. (1999) Physicochemical characterization and purification of cationic lipoplexes, *J. Phys. Chem. B* 7, 341–353.
- Murzyn, K., Róg, T., and Pasenkiewicz-Gierula, M. (2005) Phosphatidylethanolamine-phosphatidylglycerol bilayer as a model of the inner bacterial membrane, *Biophys. J.* 88, 1091–1103.
- Rytömaa, M., and Kinnunen, P. K. J. (1996) Dissociation of cytochrome *c* from liposomes by histone H1. Comparison with basic peptides, *Biochemistry* 35, 4529–4539.
- Hinderliter, A., Almeida, P. F. F., Creutz, C. E., and Biltonen, R. L. (2001) Domain formation in a fluid mixed lipid bilayer modulated through binding of the C2 protein motif, *Biochemistry* 40, 4181–4191.
- Zhao, H., Rinaldi, A. C., Di Giulio, A., Simmaco, M., and Kinnunen, P. K. J. (2002) Interactions of the antimicrobial peptides temporins with model biomembranes. Comparison of temporins B and L, *Biochemistry* 41, 4425–4436.

30. Hinderliter, A., Biltonen, R. L., and Almeida, P. F. F. (2004) Lipid modulation of protein-induced membrane domains as a mechanism for controlling signal transduction, *Biochemistry* 43, 7102–7110.
31. Meers, P., Daleke, D., Hong, K., and Papahadjopoulos, D. (1991) Interactions of annexins with membrane phospholipids, *Biochemistry* 30, 2903–2908.
32. Rueping, M., Mahajan, Y. R., Jaun, B., and Seebach, D. (2004) Design, synthesis and structural investigations of a β -peptide forming a 3_14 -helix stabilized by electrostatic interactions, *Chem.—Eur. J.* 10, 1607–1615.
33. Seebach, D., Beck, A. K., Bierbaum, D. (2004) The world of β - and γ -peptides comprised of homologated proteinogenic amino acids and other components, *Chem. Biodiversity* 1, 1111–1239.
34. Hope, M. J., Nayar, R., Mayer, L. D., and Cullis, P. R. (1993) Reduction of liposome size and preparation of unilamellar vesicles by extrusion techniques, in *Liposome Technology*, 2nd ed., (Gregoriadis, G., Ed.) Vol. I, 124–130, CRC Press, Boca Raton, FL.
35. Berclaz, N., Müller, M., Walde, P., and Luisi, P. L. (2001) Growth and transformation of vesicles studied by ferritin labeling and cryotransmission electron microscopy, *J. Phys. Chem. B* 105, 1056–1064.
36. Cho, W., Bittova, L., and Stahelin, R. V. (2001) Membrane binding assays for peripheral proteins, *Anal. Biochem.* 296, 153–161.
37. White, S. H., Wimley, W. C., Ladokhin, A. S. and Hristova, K. (1998) Protein folding in membranes: determining energetics of peptide-bilayer interactions, *Methods Enzymol.* 295, 62–87.
38. Seelig, J. (2004) Thermodynamics of lipid-peptide interactions, *Biochim. Biophys. Acta* 1666, 40–50.
39. Lazaridis, T. (2005) Implicit solvent simulations of peptide interactions with anionic lipid membranes, *Proteins: Struct., Funct., Bioinf.* 58, 518–527.
40. Beschiaschvili, G., and Seelig, J. (1990) Peptide binding to lipid bilayers. Binding isotherms and ζ -potential of a cyclic somatostatin analogue, *Biochemistry* 29, 10995–1000.
41. Cornell, B. A., Middlehurst, J. and Separovic, F. (1980) The molecular packing and stability within highly curved phospholipid bilayers, *Biochim. Biophys. Acta* 598, 405–410.
42. Ziegler, A., Blatter, X. L., Seelig, A., and Seelig, J. (2003) Protein transduction domains of HIV-1 and SIV TAT interact with charged lipid vesicles. Binding mechanism and thermodynamic analysis, *Biochemistry* 42, 9185–9194.
43. Eisenberg, M., Gresalfi, T., Riccio, T., and McLaughlin, S. (1979) Adsorption of monovalent cations to bilayer membranes containing negative phospholipids, *Biochemistry* 18, 5213–5223.
44. Seebach, D., Overhand, M., Kühnle, F. N. M., Martinoni, R., Oberer, L., Hommel, U., and Widmer, H. (1996) Synthesis by Arndt-Eistert homologation with concomitant peptide coupling. Structure determination by NMR and CD spectroscopy and by X-ray crystallography. Helical secondary structure of a β -hexapeptide in solution and its stability towards pepsin, *Helv. Chim. Acta* 79, 913–941.
45. Seebach, D., Ciceri, P., Overhand, M., Juan, B., Rigo, D., Oberer, L., Hommel, U., Amstutz, R., and Widmer, H. (1996) Probing the helical secondary structure of short-chain β -peptides, *Helv. Chim. Acta* 79, 2043–2066.
46. Frackenpohl, J., Arvidsson, P. I., Schreiber, J. V., and Seebach, D. (2001) The outstanding biological stability of β - and γ -peptides toward proteolytic enzymes: An in vitro investigation with fifteen peptidases, *ChemBioChem* 2, 445–455.
47. Wiegand, H., Wirz, B., Schweitzer, A., Camenisch, G. P., Perez, M. I. R., Gross, R., Woessner, R., Voges, R., Arvidsson, P. I., Frackenpohl, J., and Seebach, D. (2002) The outstanding metabolic stability of a C-14-labeled β -nonapeptide in rats – in vitro and in vivo pharmacokinetic studies, *Biopharm. Drug Dispos.* 23, 251–262.
48. Arvidsson, P., Ryder, N., Weiss, M., Gross, G., Kretz, O., Woessner, R., and Seebach, D. (2003) Antibiotic and hemolytic activity of a β^2/β^3 -peptide capable of folding into a 12/10-helical secondary structure, *ChemBioChem* 4, 1345–1347.
49. Sakai, N., and Matile, S. (2003) Anion-mediated transfer of polyarginine across liquid and bilayer membranes, *J. Am. Chem. Soc.* 125, 14348–14356.
50. Thorén, E. G., Persson, D., Lincoln, D., and Nordén, B. (2005) Membrane destabilizing properties of cell-penetrating peptides, *Biophys. Chem.* 114, 169–179.
51. Ladokhin, A. S., Isas, J. M., Haigler, H. T., and White, S. H. (2002) Determining the membrane topology of proteins: insertion pathway of a transmembrane helix of annexin 12, *Biochemistry* 41, 13617–13626.
52. Holopainen, J. M., Saily, M., Caldentey, J., and Kinnunen, P. K. J. (2000) The assembly factor P17 from bacteriophage PRD1 interacts with positively charged lipid membranes, *Eur. J. Biochem.* 267, 6231–6238.
53. Schendel, S. L., and Cramer, W. A. (1994) On the nature of the unfolded intermediate in the in vitro transition of the colicin E1 channel domain from the aqueous to the membrane phase, *Protein Sci.* 3, 2272–2279.
54. Zasloff, M. (2002) Antimicrobial peptides of multicellular organisms, *Nature* 415, 389–395.
55. Kim, J., Mosior, M., Chung, L. A., Wu, H., and McLaughlin, S. (1991) Binding of peptides with basic residues to membranes containing acidic phospholipids, *Biophys. J.* 60, 135–148.
56. Hartmann, W., and Galla, H. J. (1978) Binding of polylysine to charged bilayer membranes: Molecular organization of a lipid-peptide complex, *Biochim. Biophys. Acta* 509, 474–490.
57. Thorén, P. E. G., Persson, D., Esbjörner, E. K., Goksör, M., Lincoln, P., and Nordén, B. (2004) Membrane binding and translocation of cell-penetrating peptides, *Biochemistry* 43, 3471–3489.
58. Murray, D., Arbuzova, A., Hangyas-Mihalyné, G., Gambhir, A., Ben-Tal, N., Honig, B., and McLaughlin, S. (1999) Electrostatic properties of membranes containing acidic lipids and adsorbed basic peptides: Theory and experiment, *Biophys. J.* 77, 3176–3188.
59. Freire, E., Markello, T., Rigell, C., and Holloway, P. W. (1983) Calorimetric and fluorescence characterization of interactions between cytochrome b5 and phosphatidylcholine bilayers, *Biochemistry* 22, 1675–1680.
60. Matsuzaki, K., Sugishita, K., Ishibe, N., Ueha, M., Nakata, S., Miyajima, K., and Eband, R. M. (1998) Relationship of membrane curvature to the formation of pores by magainin 2, *Biochemistry* 37, 11856–11863.
61. Eband, R. F., Raguse, T. L., Gellman, S. H., and Eband, R. M. (2004) Antimicrobial 14-helical β -peptides: Potent bilayer disrupting agents, *Biochemistry* 43, 9527–9535.
62. Medina, M. L., Chapman, B. S., Bolender, J. P., and Plesniak, L. A. (2002) Transient vesicle leakage initiated by a synthetic apoptotic peptide derived from the death domain of neurotrophin receptor, p75NTR, *J. Pept. Res.* 59, 149–158.

BI060285D